Naringin attenuates renal interstitial fibrosis by regulating the TGF-β/Smad signaling pathway and inflammation

RUICHEN WANG[1,2*], GAOLEI WU[3*], TIANTIAN DAI[2], YITIAN LANG[2], ZHONGCHAO CHI[2], SHILEI YANG[1] and DESHI DONG[1,2]

[1]Department of Pharmacy, The First Affiliated Hospital of Dalian Medical University, Dalian, Liaoning 116011; [2]Department of Clinical Pharmacology, College of Pharmacy, Dalian Medical University, Dalian, Liaoning 116044; [3]Department of Pharmacy, Dalian Municipal Women and Children's Medical Center, Dalian, Liaoning 116037, P.R. China

Received February 19, 2020; Accepted July 7, 2020

DOI: 10.3892/etm.2020.9498

Abstract. Interstitial fibrosis is a typical feature of all progressive renal diseases. The process of fibrosis is frequently coupled with the presence of pro-fibrotic factors and inflammation. Naringin is a dihydroflavone compound that has been previously reported to exhibit anti-fibrotic effects in the liver, where it prevents oxidative damage. In the present study, a rat model of renal interstitial fibrosis and fibrosis cell model were established to evaluate the effects of naringin on inflammatory proteins and fibrosis markers in kidney of rats and NRK-52E cells, and to elucidate the role of the TGF-β/Smad signaling pathway in this mechanism. Compared with those in fibrotic NRK-52E cells that were stimulated by transforming growth factor-β (TGF-β), gene expression levels of α-smooth muscle actin (α-SMA), collagen 1 (COL1A1), collagen 3 (COL3A1), interleukin (IL)-1β, IL-6 and tumor necrosis factor-α (TNF-α) were all found to be significantly decreased in fibrotic NRK-52E cells following treatment with naringin (50, 100 and 200 ng/ml). Results from the histopathological studies showed that naringin treatment preserved the renal tissue structure and reduced the degree of fibrosis in the kidney tissues of rats that underwent unilateral ureteral obstruction (UUO). In addition, naringin administration reduced the expression of α-SMA, COL1A1, COL3A1, IL-1β, IL-6 and TNF-α in the kidneys of rats following UUO. The current study, using western blot analysis, indicated that naringin also downregulated the activation of Smad2/3 and the expression of Smad4, high-mobility group protein B1, activator protein-1, NF-κB and cyclooxygenase-2 whilst upregulating the expression of Smad7 in fibrotic NRK-52E cells and rats in the UUO group. In conclusion, naringin could antagonize renal interstitial fibrosis by regulating the TGF-β/Smad pathway and the expression of inflammatory factors.

Correspondence to: Dr Deshi Dong or Dr Shilei Yang, Department of Pharmacy, The First Affiliated Hospital of Dalian Medical University, 222 Zhongshan Road, Dalian, Liaoning 116011, P.R. China
E-mail: dongdeshi@dmu.edu.cn
E-mail: yangshi_lei@163.com

*Contributed equally

Key words: naringin, renal interstitial fibrosis, anti-inflammatory, transforming growth factor-β/Smad

Introduction

Renal fibrosis is a frequent occurrence during the deterioration of chronic kidney diseases into end-stage renal disease (1). It is a chronic clinical disease that is characterized by the formation of superfluous fibrous connective tissues, gradual reduction in glomerular filtration and the gradual decline in renal tubular function (2). In addition to chronic kidney diseases, other factors can also lead to renal fibrosis, including systemic lupus erythematosus, genetic factors, diabetes, hypertension, drugs, hepatitis B, immune deficiency and kidney transplantation. At present, the incidence of chronic kidney disease is between 6.6 and 13% in China (3). Renal interstitial fibrosis (RIF) and glomerulosclerosis are two principal features of renal fibrosis (4). Compared with glomerulosclerosis, RIF holds higher research significance since renal interstitial lesions can be used as an indicator of the severity of decline in renal function (4). The pathological features of renal damage during RIF are mainly reflected by the observed accumulation of cells and collagen, atrophy and dilation of renal tubules and the loss of renal tubules and interstitial capillaries (5). Therefore, it remains urgent to investigate the mechanism underlying the RIF process.

RIF is a complex biological process that involves a variety of cytokines, signaling pathways and processes, including inflammation, apoptosis and oxidative stress (6). At present, the precise molecular mechanism underlying renal fibrosis remains poorly understood. Renal fibrosis has been previously reported to involve a multitude of signaling pathways, including transforming growth factor (TGF)-β/Smad (7), apoptosis signal-regulating kinase (8), 5'AMP-activated protein kinase/NADPH oxidase 4 (9) and the Janus kinase/STAT/glycogen synthase kinase-3β/β-catenin (10) pathways. Regardless of the etiology, high levels of TGF-β activation have been frequently associated with fibrosis

and disease progression (11). It has been previously reported that the NF-κB family of transcription factors can promote the expression of TGF-β, leading to the activation of the TGF-β/Smad pathway to mediate downstream physiological effects (12). Smad proteins are intracellular effectors of TGF-β (13). Smad4 is a key regulator in the Smad protein family that can interact with Smad7 and Smad3 to modulate their transcriptional activities, upstream of the renal inflammatory and fibrotic processes (14). It has also been previously demonstrated that dysregulation of the TGF-β/Smad pathway is an important cause of tissue fibrosis (11). TGF-β1 can upregulate the expression of Smad2 and Smad3 during tissue fibrosis, a process that is negatively regulated by Smad7 as part of a negative feedback loop (15). By contrast, previous studies have demonstrated that the long-term persistence of inflammatory factors, such as tumor necrosis factor-α (TNF-α) and interleukin-1β (IL-1β), in renal tissues were closely associated with RIF, which sensitizes the kidney cells to TGF-β to aggravate fibrosis further (16,17). Of note, macrophages are the main type of infiltrating immune cells that have been found to mediate this inflammatory process (18). The kidney produces a large number of monocytes/macrophages, which constantly infiltrates the kidney to produce pro-inflammatory cytokines, including TNF-α and IL-1β, to induce kidney inflammation (19). It has been previously reported that inhibiting the release of inflammatory factors can attenuate the progress of RIF. These previous observations aforementioned suggest that the TGF-β/Smad pathway and inflammatory proteins serve important roles in the development of RIF.

Naringin is a dihydroflavonoid that can be found in the immature or near-mature dry outer pericarp of pomelo, grapefruit and the citrus of *Rutaceae* (20,21). A number of studies have previously demonstrated that naringin exhibits several biologically active effects, including anti-inflammation, hepato-protection, anti-apoptosis, antioxidant in addition to inhibiting genetic toxicity (22-25). Naringin can effectively inhibit carbon tetrachloride-induced acute liver and kidney injury in mice by serving as an antioxidant and scavenging free radicals (26). Additionally, it has been previously shown that naringin can alleviate sodium arsenite-induced liver fibrosis in rats by suppressing TGF-β (27,28). However, the potential effects of naringin on RIF remain poorly understand. Therefore, a rat model of renal interstitial fibrosis and a fibrosis cell model was established to evaluate the effects of naringin on inflammatory proteins and fibrosis markers in kidney of rats and NRK-52E cells, and to elucidate the mechanism governing this.

Materials and methods

Materials and reagents. Naringin was purchased from Dalian Meilun Biotech Co., Ltd. FBS was purchased from Hyclone, Cytiva. TGF-β was purchased from ProteinTech Group, Inc. Cell proliferation Kit I MTT (cat. no. 11465007001) was purchased from Roche Diagnostics. DAPI, DMEM, Tween-20 and 5% skimmed milk powder were purchased from Beijing Solarbio Science & Technology Co., Ltd. Blood urea nitrogen (BUN; cat. no. C013-2) and creatinine (Scr) kits (cat. no. C011-1) were purchased from Nanjing Jiancheng Bioengineering Institute. Bicinchoninic acid (BCA) protein concentration determination and tissue protein extraction kits were purchased from Beyotime Institute of Biotechnology. Anti-α-smooth muscle actin (α-SMA; cat. no. BM0002) antibody used for immunofluorescence was purchased from Wuhan Boster Biological Technology, Ltd. Anti-phosphorylated (p)-Smad2/3 (cat. no. WL02305), Smad7 (cat. no. WL02975), α-SMA (cat. no. WL02510) and NF-κB (cat. no. WL01980) were purchased from Wanleibio Co., Ltd. Anti-collagen 1 (COL1A1; cat. no. 14695-1-AP), TGF-β (cat. no. 21898-1-AP), Smad2 (cat. no. 12570-1-AP), Smad3 (cat. no. 25494-1-AP), Smad4 (cat. no. 51144-1-AP), cyclooxygenase (COX)-2 (cat. no. 12375-1-AP), activator protein-1 (AP-1; cat. no. 22114-1-AP), high-mobility group protein B1 (HMGB1; cat. no. 10829-1-AP), GAPDH (cat. no. 10494-1-AP), HRP-conjugated Affinipure Goat Anti-Rabbit IgG (H+L) (secondary antibody, cat. no. SA00001-2), fluorescent anti body and chemiluminescence Western Blot kit (cat. no. B500034) were purchased from Wuhan Sanying Biotechnology (https://www.ptgcn.com/).

Experimental cells. The rat renal tubular epithelial cell line NRK-52E was purchased from the Institute of Biochemistry and Cell Biology, Shanghai Academy of Life Sciences, Chinese Academy of Sciences. NRK-52E cells were incubated in DMEM containing 10% FBS under 5% CO_2 and 37˚C.

MTT assay. NRK-52E cells were seeded into 96-well plates at a concentration of $5x10^4$ cells/ml. Different concentrations of naringin (0, 50, 100, 200, 400 and 800 ng/ml) were then added to the cells. After 24 h incubation at 37˚C 50 μl serum-free media and 50 μl MTT reagent were added into each well (29). After incubation at 37˚C, the MTT reagent-supplemented media was removed and 150 μl solubilization solution was added into each well. The plates were then shaken on an orbital shaker for 15 min at 37˚C before absorbance at 590 nm was read for each well, which was used to calculate the cell survival rate. The formula used was $\%viable\ cells=Absorbance_{sample}-Absorbance_{blank}) x100/(Absorbance_{control}-Absorbance_{blank})$.

For TGF-β treatment, NRK-52E cells at a concentration of $1x10^5$/ml were seeded into 96-well plates. After 24 h of culture at 37˚C, cells in the blank group were incubated with DMEM without FBS, whilst those in the model group was provided with TGF-β (10 ng/ml). Cells in the treatment group were treated with TGF-β (10 ng/ml) and naringin at different concentrations (50, 100 and 200 ng/ml) for 24 h at 37˚C, following which MTT assay was used to calculate the cell survival rate.

Experimental animals. A total of 36 Male Sprague-Dawley (SD) rats of 7-weeks old weighing 200-220 g were purchased from the SPF Experimental Animal Center of Dalian Medical University (permit no. SCXK 2013-0003; Dalian, China). Rats were housed in an animal room under a 12-h light/dark cycle, at 20˚C and 60% relative humidity, and were provided with food and drink *ad libitum*. Rats were acclimatized for 1 week and fasted for 12 h before each experiment (30,31). All rat experiments were conducted in accordance with the National Institutes of Health guide for the care and use of Laboratory animals (NIH Publications no. 85-23, revised 1985) (32). All efforts were made to minimize the number of animals used and their suffering.

A total of 36 SD rats were divided into the following groups (n=6): i) Sham group; ii) UUO group; iii) high dose naringin administration group (80 mg/kg); iv) medium dose naringin administration group (40 mg/kg); v) low dose naringin administration group (20 mg/kg); and vi) single naringin administration group (80 mg/kg).

RIF was induced by unilateral ureteral obstruction (UUO) in rats (33,34). The operation procedure was as follows: Rats were fasted for 12 h prior to operation but have free access to drinking water. Rats were fixed on the operating table following anesthesia with pentobarbital (60 mg/kg intraperitoneal injection). After sterilization and shaving, a longitudinal incision was made on the left side of the abdomen and the left kidney and ureter were exposed. Rats in the UUO groups were achieved by ligating the left ureter with 3-0 silk through a left lateral incision. The abdomen was finally sutured in layers. The left ureter was exposed but not ligated in the sham-operated or the single administration groups. On day 2 after operation, rats in the high, middle, low dose administration groups and the single administration group were given naringin daily by intragastrical administration for 28 consecutive days. The sham-operated and model groups received an equivalent volume of 0.5% CMC-Na. Rats were then fasted overnight and fixed in a supine position on the operating table on day 28 before blood samples were collected from abdominal aorta from rats after anesthesia with pentobarbital (60 mg/kg intraperitoneal injection). Blood samples were placed in heparin tubes and immediately centrifuged at 4,000 x g for 10 min at 4˚C. The levels of BUN and Scr were calculated according to the manufacturer's protocol. After sacrificing the rats, the left kidney was quickly excised, decapsulated and immediately placed into oxygenated buffer at 4˚C and then split into two halves. One part of the kidney tissue was stored at -20˚C until further biochemical testing whereas the other part was fixed for 1 week in 10% formaldehyde solution at 25˚C for histopathological examination.

Histopathological examination. According to the routine method of histopathology, kidney samples fixed in 10% formaldehyde solution (pH 7.2) were embedded in paraffin to make wax blocks. Using a rotatory microtome, 4-μm thick kidney tissue sections were prepared for histopathological examination. Histopathological analysis was conducted under an light microscope (magnification, x400) after hematoxylin and eosin staining (H&E), Masson's trichrome staining and Sirius red staining (all, Wuhan Servicebio Technology Co., Ltd.). The protocol for H&E staining is briefly described as follows: Slices were stained with hematoxylin for 10 min at 25˚C and then dehydrated in 85 and 95% ethanol for 4 min, before being stained with eosin for 4-5 min at 25˚C and dehydrated again using three cylinders of 100% anhydrous ethanol. Slices were washed with n-butanol and xylene before sealing with neutral gum. The protocol for Masson's trichrome staining is briefly described as follows: Slices were immersed in Masson solution A overnight at 25˚C before incubation in Masson solution A at a 65˚C for 30 min. The slices were then immersed in mixed dye solution for 1 min, differentiated with 1% hydrochloric acid alcohol for ~1 min and incubated in Masson solution D for 6 min at 25˚C. Incubation in Masson solution E for 1 min and Masson solution F for 8-15 sec at 25˚C then ensued, before the slices were sealed after dehydration with anhydrous ethanol. The protocol for Sirius red staining is briefly described as follows: Slices were immersed in Sirius red solution for 8 min at 25˚C and dehydrated by anhydrous ethanol. Slices were washed with xylene and sealed with neutral gum.

Immunofluorescence analysis α-SMA. NRK-52E cells were collected and seeded into six-well plates at $1x10^5$ cells/ml. After 24 h at 37˚C, the blank group was replaced with DMEM without FBS, the model group was treated with TGF-β (10 ng/ml), whilst the other groups were treated with TGF-β (10 ng/ml) and naringin (50, 100 and 200 ng/ml) for 24 h at 37˚C. Cells were rinsed three times with PBS, fixed at room temperature in 10% formaldehyde for 20 min and incubated with 0.2% Triton X-100 for 10 min. The cells were then treated with the immunofluorescence blocking solution for 1 h at 25˚C and incubated overnight with the anti-α-SMA antibody (1:50) at 4˚C. Rhodamine-conjugated fluorescent secondary antibody IgG h + L (1:70) was subsequently added and incubated at 37˚C for 1 h. Cells were washed three times with PBS before DAPI (10 g/ml) was added and incubated at 37˚C for 10 min. Cells were washed and imaged at x400 magnification using an inverted fluorescence microscope.

For tissue sections, they were first washed in xylenes, followed by 2x10 min and then washed in 100% ethanol for 5 min, washed in 95% ethanol for 5 min, washed in 90% ethanol for 5 min, washed in 80% ethanol for 5 min, washed in 70% ethanol for 5 min and washed in water for 5 min. Antigens were retrieved and the sections were sealed using immunofluorescent blocking solution at 25˚C. After PBS cleaning, the sections were incubated with anti-α-SMA antibody (1:70) overnight at 4˚C before being washed three times with PBS and incubated with fluorescein-conjugated secondary antibodies (1:70) at 37˚C for 1 h. DAPI (10 g/ml) was then added and incubated at 37˚C for 10 min. The sections were finally imaged at x400 magnification using a fluorescence microscope.

Reverse transcription-quantitative PCR. Total RNA was extracted from renal and NRK-52E cells using RNAiso Plus® Reagent Kit according to manufacturer's protocol (Takara Biotechnology Co., Ltd.) and then reverse-transcribed into cDNA using PrimeScript™ RT Reagent kit with DNA Eraser (Takara Biotechnology Co., Ltd.). The cDNA was amplified using SYBR® Premix Ex Taq™ kit (Takara Biotechnology Co., Ltd.). Primer sequences are shown in Table I. The thermocycling conditions of RT PCR were as follows: Initial denaturation at 95˚C for 30 sec, followed by 40 cycles of 95˚C for 5 sec and 60˚C for 30 sec, dissociation at 95˚C for 15 sec and 60˚C for 60 sec and 95˚C for 15 sec. qPCR was subsequently performed using SYBR-Green PCR Master Mix in an ABI prism 7500 Sequence Detection System (Applied Biosystems; Thermo Fisher Scientific, Inc.). The thermocycling conditions of qPCR were as follows: Initial denaturation at 95˚C for 5 min, followed by 40 cycles of 95˚C for 5 sec and 60˚C for 30 sec, dissociation at 95˚C for 15 sec and 60˚C for 60 sec and 95˚C for 15 sec. The $2^{-\Delta\Delta Cq}$ method was used to calculate the fold change for each gene relative to that of GAPDH (35).

Protein isolation and western blotting assay. NRK-52E cells and kidney tissues were utilized to extract proteins by

Table I. Primers used for reverse transcription-quantitative PCR.

Gene	Forward primer (5'-3')	Reverse primer (5'-3')
Rat-GAPDH	GAAAGACAACCAGGCCATCAG	TCATGAATGCATCCTTTTTTGC
Rat-IL-1β	CCCTGAACTCAACTGTGAAATAGCA	CCCAAGTCAAGGGCTTGGAA
Rat-IL-6	ATTGTATGAACAGCGATGATGCAC	CCAGGTAGAAACGGAACTCCAGA
Rat-TNF-α	TCAGTTCCATGGCCCAGAC	GTTGTCTTTGAGATCCATGCCATT
Rat-α-SMA	AGCCAGTCGCCATCAGGAAC	GGGAGCATCATCACCAGCAA
Rat-COL1A1	GACATGTTCAGCTTTGTGGACCC	AGGGACCCTTAGGCCATTGTGTA
Rat-COL3A1	TTTGGCACAGCAGTCCAATGTA	GACAGATCCCGAGTCGCAGA

IL, interleukin; COL, collagen; TNF-α, tumor necrosis factor-α; α-SMA, α-smooth muscle actin.

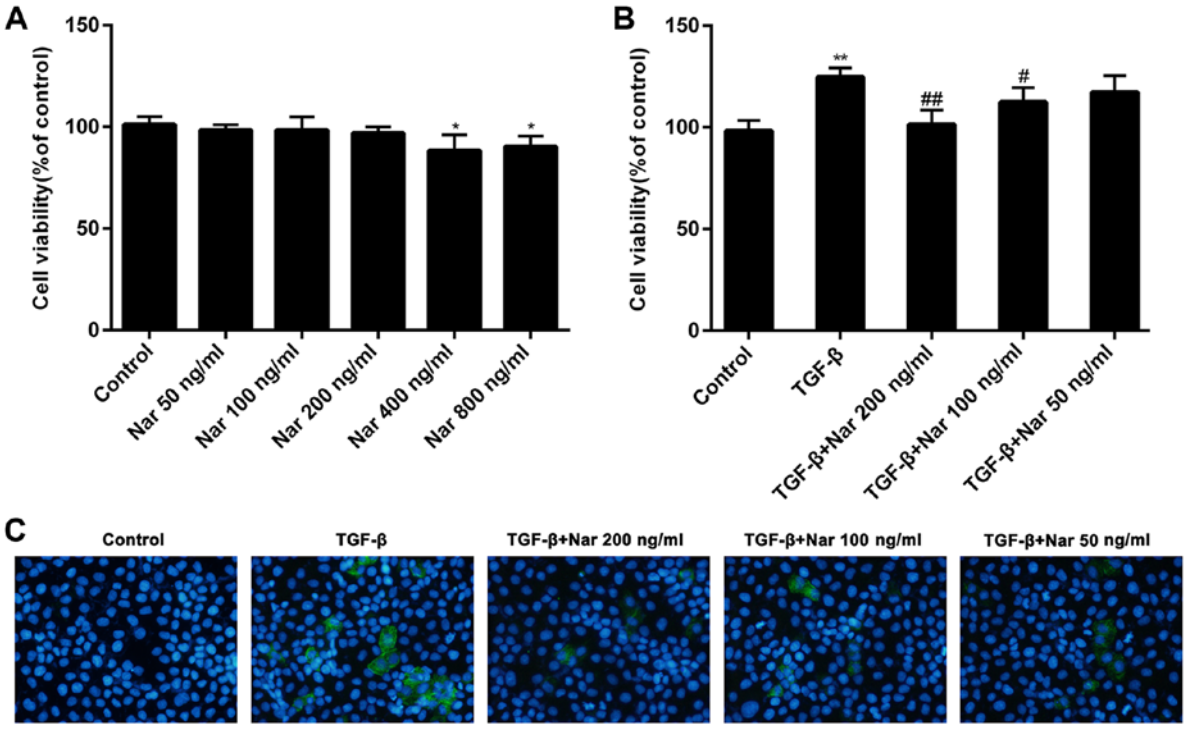

Figure 1. Effect of naringin on the fibrosis of NRK-52E cells induced by TGF-β. (A) Toxicity of naringin on NRK-52E cells. (B) The effect of naringin on NRK-52E cell viability following treatment with TGF-β. (C) The effect of naringin on α-SMA expression in NRK-52E cells following treatment with TGF-β as examined by immunofluorescence. Magnification, x400. Data is presented as the mean ± SD (n=6). *P<0.05, **P<0.01 vs. Control; $^{\#}$P<0.05 and $^{\#\#}$P<0.01 vs. TGF-β. Nar, naringin; TGF-β, transforming growth factor-β.

homogenization in RIPA Buffer (cat. no. R0278; Sigma-Aldrich; Merck KGaA) buffer containing PMSF (Beyotime Institute of Biotechnology). Protein concentration was determined using the BCA kit. Protein samples (30 μg) were separated by 10% SDS-PAGE and transferred onto PVDF membranes (Immobilon-P; EMD Millipore). Anti-Smad2/3, Smad7, α-SMA, NF-κB, TGF-β, Smad2, Smad3, Smad4, COX-2, AP-1 and HMGB1 antibodies (all, 1:2,000) were incubated overnight at 4˚C. GAPDH (1:3,000) were incubated for 2 h at 4˚C as the secondary antibody. The protein bands were visualized using a chemiluminescence Western Blot kit and identified using the ChemiDoc™ XRS and Imaging system (Bio-Rad Laboratories, Inc.). Quantification of protein expression was performed using the Image Lab™ Software (version 4.0.1 build 6; Bio-Rad Laboratories, Inc.).

Statistical analysis. The experimental data were presented as the mean ± SD (n=6 for rats; n=6 for cells). To test for statistically significant differences among multiple treatments for a given parameter, One-way ANOVA followed by Tukey's multiple comparisons test was performed using the GraphPad Prism version 5.00 software (GraphPad Software, Inc.).

Results

Naringin reduces NRK-52E cell viability induced by TGF-β. To investigate the toxicity of naringin on NRK-52E cells, ascending concentrations of naringin (0, 50, 100, 200, 400 and 800 ng/ml) were incubated with NRK-52E cells for 24 h. Naringin exerted little or no toxicity on NRK-52E cells at concentrations of <200 ng/ml (Fig. 1A). It was also found

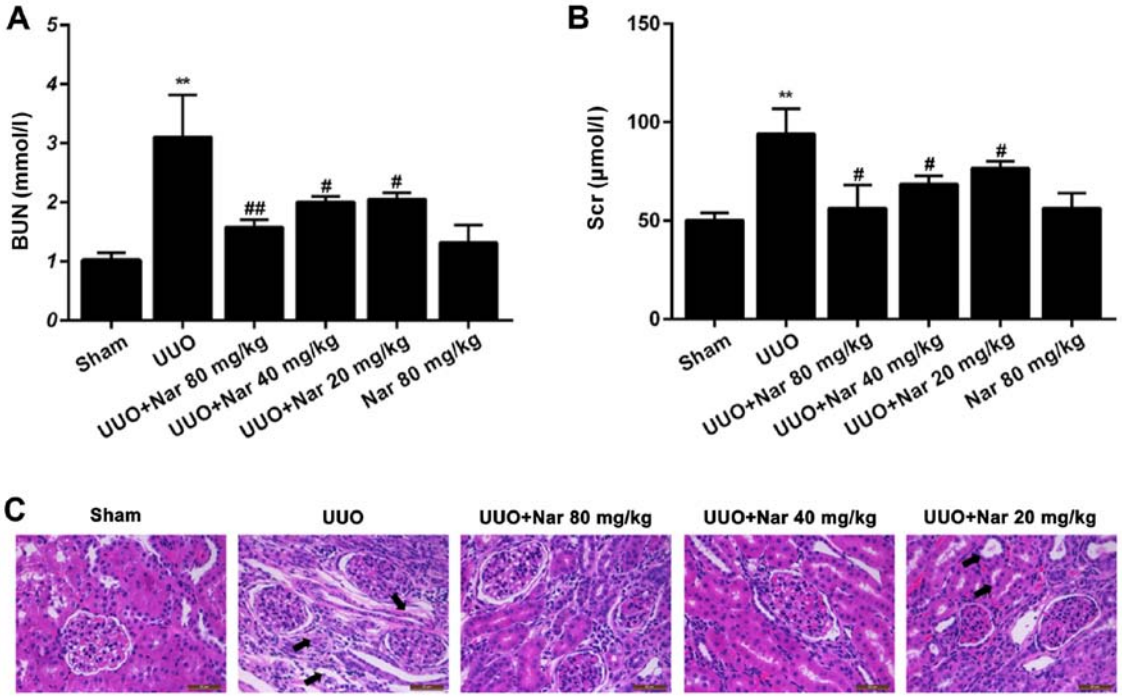

Figure 2. Effect of naringin on renal interstitial fibrosis induced by UUO in renal cortex of rats. Effect of naringin treatment on (A) BUN and (B) Scr levels. (C) Effect of 20, 40 and 80 mg/kg naringin on renal sections as assessed using H&E staining. Magnification, x400. Data is presented as mean ± SD (n=6). **P<0.01 vs. Sham; $^{\#}$P<0.05, $^{\#\#}$P<0.01 vs. UUO. Nar, naringin; UUO, unilateral ureteral obstruction; BUN, blood urea nitrogen; Scr, serum creatinine.

that naringin (100 and 200 ng/ml) could significantly reduce the viability of NRK-52E cells induced by TGF-β (Fig. 1B). These results suggest that naringin can reverse the potentiating effects of TGF-β on NRK-52E cell viability. Naringin at concentrations of 50, 100 and 200 ng/ml was therefore chosen for subsequent experiments.

Inhibitory effects of naringin on cell fibrosis induced by TGF-β. To investigate the effect of naringin on cell fibrosis induced by TGF-β, the expression of fibrotic markers α-SMA was detected by immunofluorescence. Compared with cells treated with TGF-β alone, the expression levels of α-SMA protein in NRK-52E cells treated with naringin (50, 100 and 200 ng/ml) was found to be markedly reduced (Fig. 1C). These results indicated that naringin could effectively inhibit cell fibrosis induced by TGF-β.

Effect of naringin on renal function in rats with RIF induced by UUO. To investigate the effect of naringin on renal function in rats following UUO, blood samples were collected for BUN and Scr analysis. Compared with those in the control group, BUN and Scr levels were demonstrated to be significantly increased in the UUO group (Fig. 2A and B). Compared with those in the UUO group, BUN levels were demonstrated to be significantly reduced, specifically by 49.1, 35.4 and 33.9% in the high, middle and low dose groups, respectively (Fig. 2A). Similarly. Scr levels were also significantly decreased, by 40.1, 27.2 and 18.5%, respectively, compared with those in the UUO groups (Fig. 2B). These findings suggested that the levels of BUN and Scr can be significantly reduced after naringin treatment in UUO rats. There was no significant difference in the levels of BUN and Scr between those in the single naringin administration and sham groups, suggesting that naringin 80 mg/kg exerted no adverse effects on the renal function of rats.

Effect of naringin on renal pathology in rats following UUO-induced RIF. To further evaluate the histological damage in the kidney tissues, the histological sections of the kidneys of rats in each group were analyzed by H&E staining. Compared with those in the sham group, some renal tubules in the UUO group were demonstrated to be dilated, atrophied and necrotized, where a large number of monocytes and lymphocytes infiltrated (Fig. 2C). Compared with tissues in the UUO group, the expansion or atrophy of the renal tubules treated with naringin (20, 40 and 80 mg/kg) were improved, where the degree of vacuolar degeneration was reduced (Fig. 2C). These results suggest that naringin can effectively improve the histopathological changes in the kidney after UUO.

Naringin inhibits RIF induced by UUO. To investigate the effects of naringin on RIF following UUO, Masson's trichrome and Sirius red staining were used to evaluate the degree of RIF in rats in each group. Compared with those in the sham group, the proliferation and deposition of collagen fibrous connective tissues in the kidney tissues of rats in the UUO group were markedly increased. By contrast, compared with tissues from the UUO group, the extent of collagen fibrous connective tissue deposition and proliferation in the kidneys of rats treated with naringin (20, 40 and 80 mg/kg) were visibly reduced (Fig. 3). The content of blue and red fibers were all shown to be reduced after treatment with naringin, with the magnitude of reduction the highest in the high dose group. In addition, results of immunofluorescence analysis showed that naringin administration could reduce the expression of α-SMA in the kidney tissues of UUO rats (Fig. 4). These

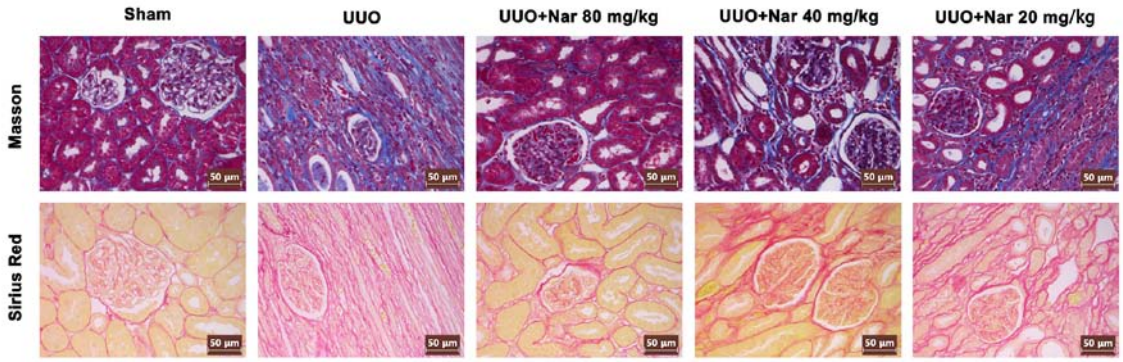

Figure 3. Effect of naringin on renal interstitial fibrosis induced by UUO in rats. Collagen and amyloid deposition in renal tissues following naringin administration was assessed using Masson's trichrome and Sirius Red staining. Magnification, x400. The length of the scale bars is 50 μm. Nar, naringin; UUO, unilateral ureteral obstruction.

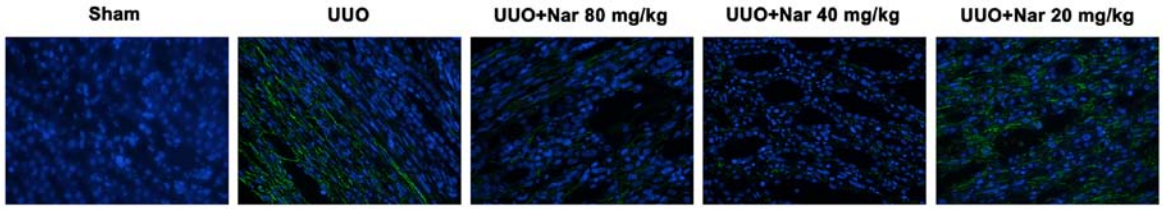

Figure 4. Effect of naringin on α-SMA expression in renal tissues following UUO in rats as examined using immunofluorescence. Magnification, x400. Nar, naringin; UUO, unilateral ureteral obstruction.

results indicated that naringin can notably reduce the degree of RIF induced by UUO.

Effect of naringin on the expression of fibrotic markers. To examine the effect of naringin on the expression of fibrotic markers in NRK-52E cells and rat kidneys, the expression of TGF-β, α-SMA and COL1A1 was next measured. The protein expression levels of TGF-β, α-SMA and COL1A1 in the NRK-52E fibrosis cell model induced by TGF-β and kidney tissues of rats following UUO were found to be significantly higher compared with those in the control group (NRK-52E) and sham group (rat models). In addition, the mRNA expression levels of α-SMA, COL1A1 and COL3A1 were revealed to be significantly reduced in NRK-52E cells and rats in the UUO group treated with naringin (Fig. 5A and C). Compared with those in the control NRK-52E cell and UUO rat groups, naringin treatment significantly reduced the expression of TGF-β, α-SMA and COL1A1 in both TGF-β-treated NRK-52E cell models and kidney tissues of rat models following UUO, respectively (Fig. 6).These results suggest that the degree of fibrosis in both the fibrotic cell and UUO rat models was improved following treatment with naringin.

Effect of naringin on the expression of components of the TGF-β/Smad pathway. To investigate the mechanism of the inhibitory effects of naringin on TGF-β-induced RIF, the effect of naringin on the expression of Smad, downstream regulators of TGF-β was subsequently investigated (Fig. 7). Compared with those in the control cell group and the sham group, the degree of Smad2/3 phosphorylation and Smad4 expression in the TGF-β-treated cell group and kidney tissues of rats in the UUO group were found to be significantly increased (Fig 7). Compared with those in the TGF-β-treated cell group or rats in the UUO group, the phosphorylation of Smad2/3 and Smad4 expression in TGF-β-treated NRK-52E cells and rats in the UUO group were significantly reduced following treatment with naringin in both models (Fig. 7). By contrast, the expression of Smad7 exhibited opposite trends in both *in vitro* and *in vivo* models. These observations suggest that naringin treatment can alleviate fibrosis by regulating the expression of Smad proteins.

Effect of naringin on the expression of inflammatory proteins. Since renal fibrosis is frequently accompanied with inflammation (36), the effect of naringin on the expression of inflammatory proteins was next investigated. Naringin treatment significantly reduced the expression of inflammatory factors TNF-α, IL-1β and IL-6 in the kidney tissues of UUO rats and TGF-β-treated NRK-52E cells (Fig. 5B and D). In addition, the expression levels of HMGB1, AP-1, NF-κB and COX-2 proteins in TGF-β-treated NRK-52E cells and kidney tissues of UUO rats were found to be significantly higher compared with those in the control cell group and sham group, respectively (Fig. 8). Naringin treatment significantly reversed the increased expression of HMGB1, AP-1, NF-κB and COX-2 in both the TGF-β-treated NRK-52E cell model and kidney tissues of UUO rats (Fig. 8). In summary, these results suggested that naringin may also reduce the degree of fibrosis by suppressing the expression of inflammatory proteins.

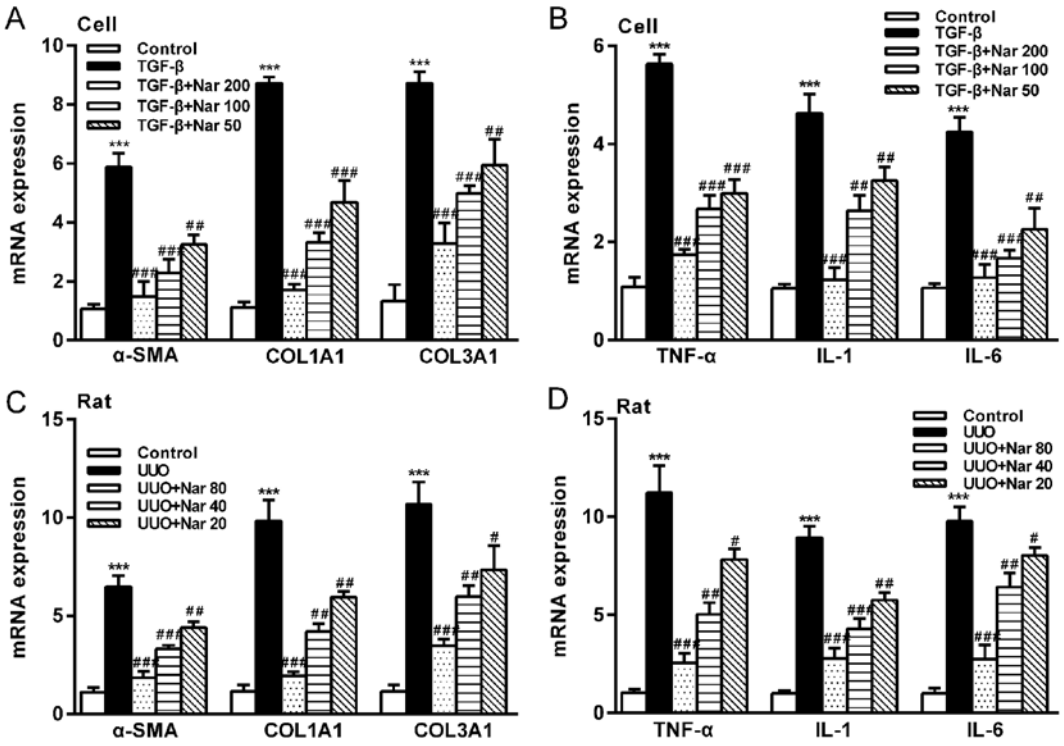

Figure 5. Effect of naringin on the mRNA expression of fibrotic markers and inflammatory factors. (A) Effect of naringin on the gene expression of α-SMA, COL1A1 and COL3A1 in NRK-52E cells. (B) Effect of naringin on the gene expression of TNF-α, IL-1 and IL-6 in NRK-52E cells. (C) Effect of naringin on gene expression of α-SMA, COL1A1 and COL3A1 in rat kidney tissues. (D) Effect of naringin on the gene expression of TNF-α, IL-1 and IL-6 in rat kidney tissues. Data is presented as the mean ± SD (n=6). ***P<0.001 vs. Control; $^{\#}$P<0.05, $^{\#\#}$P<0.01 and $^{\#\#\#}$P<0.001 vs. UUO or TGF-β. Nar, naringin; UUO, unilateral ureteral obstruction; COL, collagen; TNF-α, tumor necrosis factor-α; α-SMA, α-smooth muscle actin; IL, interleukin.

Discussion

Renal fibrosis is a frequent pathological outcome during the latter stages chronic kidney disease (37). RIF is a pathological manifestation of renal fibrosis that is regularly observed and is closely associated with reductions in renal function in patients with chronic kidney disease (38). Therefore, prevention and intervention strategies of RIF would be of great benefit for patients with chronic kidney diseases. Although considerable amount of information has been obtained regarding the underlying mechanism of renal fibrosis over the past decade, effective therapeutic methods for the prevention and treatment of RIF remain elusive. Naringin is a type of dihydroflavonoids with previously reported pharmacological effects, including antioxidant, hypolipidemic, antimicrobial, anti-inflammatory and anti-fibrotic effects in the liver (39). The present study found that naringin also exhibited anti-fibrotic effects in the rat kidney, possibly by regulating the TGF-β/Smad signaling pathway to inhibit the expression of inflammatory factors.

In the present study, the rat model of RIF was used to investigate the potential effects of naringin. There are currently three main methods used for establishing renal fibrosis in animals: i) Surgical methods, including UUO (40), 5/6 nephrectomy (41) and ischemia-reperfusion injury model (42); ii) drug or toxic induction methods, including treatment with adenine, aristolochic acid and cyclosporine, which induce renal fibrosis after long-term administration (43); and iii) compound models, including folate-*Phd14* gene knockout-induced fibrosis (44) and transgenic-KIM-1REC-tg mouse models (45). Due to potential drug interactions, drug or toxic induction methods were not used in the present study. UUO, 5/6 nephrectomy and ischemia-reperfusion models are widely applied for renal fibrosis surgery. The establishment of 5/6 nephrectomy models requires two separate operations followed by obligatory regular monitoring for ≥5 weeks (41). This procedure is highly complex, where the time of model establishment is substantially longer compared with UUO. Ischemia-reperfusion model mainly simulates the changes in renal function and renal fibrosis after renal transplantation that can be used to reflect glomerulosclerosis and RIF (42). UUO model is used to mimic RIF in a manner that is characterized by rapid pathological changes in 1-2 weeks, reduced animal mortality rates, involves operation procedures that are less complex and good reproducibility (40,46). Following successful model establishment, pathological manifestations include collagen deposition in the renal interstitium, infiltration of inflammatory cells and dilatation or atrophy of renal tubules (47). In addition, serological indicators BUN were increased 1.5-fold whilst Scr increased by 2-fold (48-50). Therefore, for the present study the UUO rat model was chosen as the animal model. According to H&E staining, compared with those in the sham group, kidney tissues of rats in the UUO group exhibited a large number of infiltrating inflammatory cells, nuclear deformation and renal tubule dilatation or atrophy. Masson's trichrome and Sirius red staining revealed large quantities of collagen deposition in the kidneys of the UUO group of rats. The serum BUN levels of rats in the UUO group was found to be three times higher compared with those in the sham group, whilst serum Scr levels was found to be 1.6 times higher compared with those in the sham group.

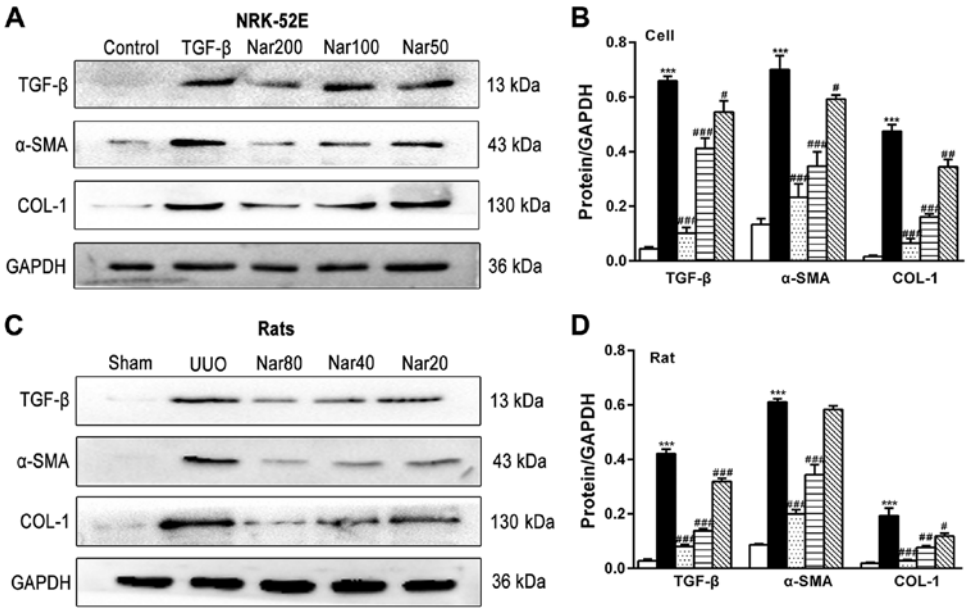

Figure 6. Effect of naringin on the protein expression of fibrotic markers in NRK-52E cells and rat kidneys. (A) Effect of naringin on TGF-β, α-SMA and COL1A1 protein expression in NRK-52E cells. (B) Quantitative analysis of the protein expression of TGF-β, α-SMA and COL1A1 in NRK-52E cells. (C) Effect of naringin on TGF-β, α-SMA and COL1A1 in rat kidneys. (D) Quantitative analysis of the protein expression of TGF-β, α-SMA and COL1A1 in rat kidneys. Data is presented as mean ± SD (n=6). ***P<0.001 vs. Control; $^{\#}$P<0.05, $^{\#\#}$P<0.01, $^{\#\#\#}$P<0.001 vs. UUO or TGF-β. Nar, naringin; UUO, unilateral ureteral obstruction; COL, collagen; TNF-α, tumor necrosis factor-α; α-SMA, α-smooth muscle actin; IL, interleukin; TGF-β, transforming growth factor-β.

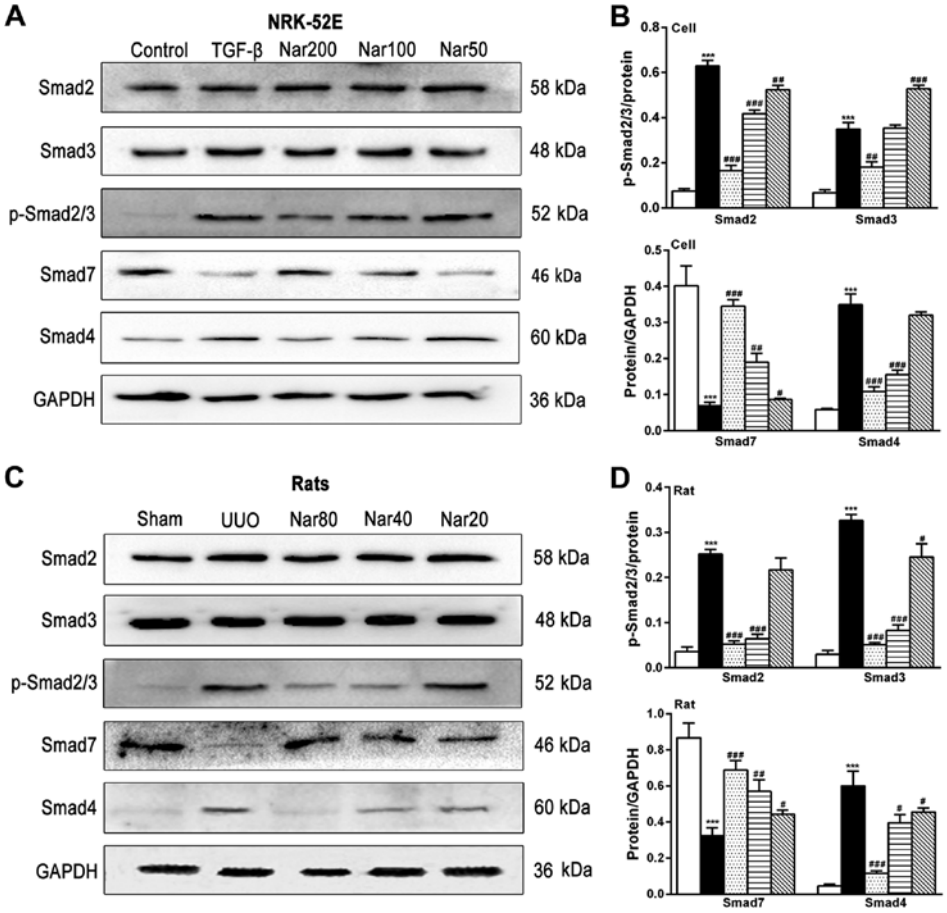

Figure 7. Effect of naringin on the expression of key components of the TGF-β/Smad pathway. (A) Effect of naringin on the protein levels of Smad2, Smad3, p-Smad2/3, Smad7 and Smad4 in NRK-52E cells. (B) Quantitative analysis of the protein levels of Smad2, Smad3, p-Smad2/3, Smad7 and Smad4 in NRK-52E cells. (C) Effect of naringin on the protein levels of Smad2, Smad3, p-Smad2/3, Smad7 and Smad4 in rat kidneys. (D) Quantitative analysis of the protein levels of Smad2, Smad3, p-Smad2/3, Smad7 and Smad4 in rat kidneys. Data is presented as mean ± SD (n=6). ***P<0.001 vs. Control; $^{\#}$P<0.05, $^{\#\#}$P<0.01 and $^{\#\#\#}$P<0.001 vs. UUO or TGF-β. Nar, naringin; UUO, unilateral ureteral obstruction; COL, collagen; TNF-α, tumor necrosis factor-α; α-SMA, α-smooth muscle actin; IL, interleukin; TGF-β, transforming growth factor-β.

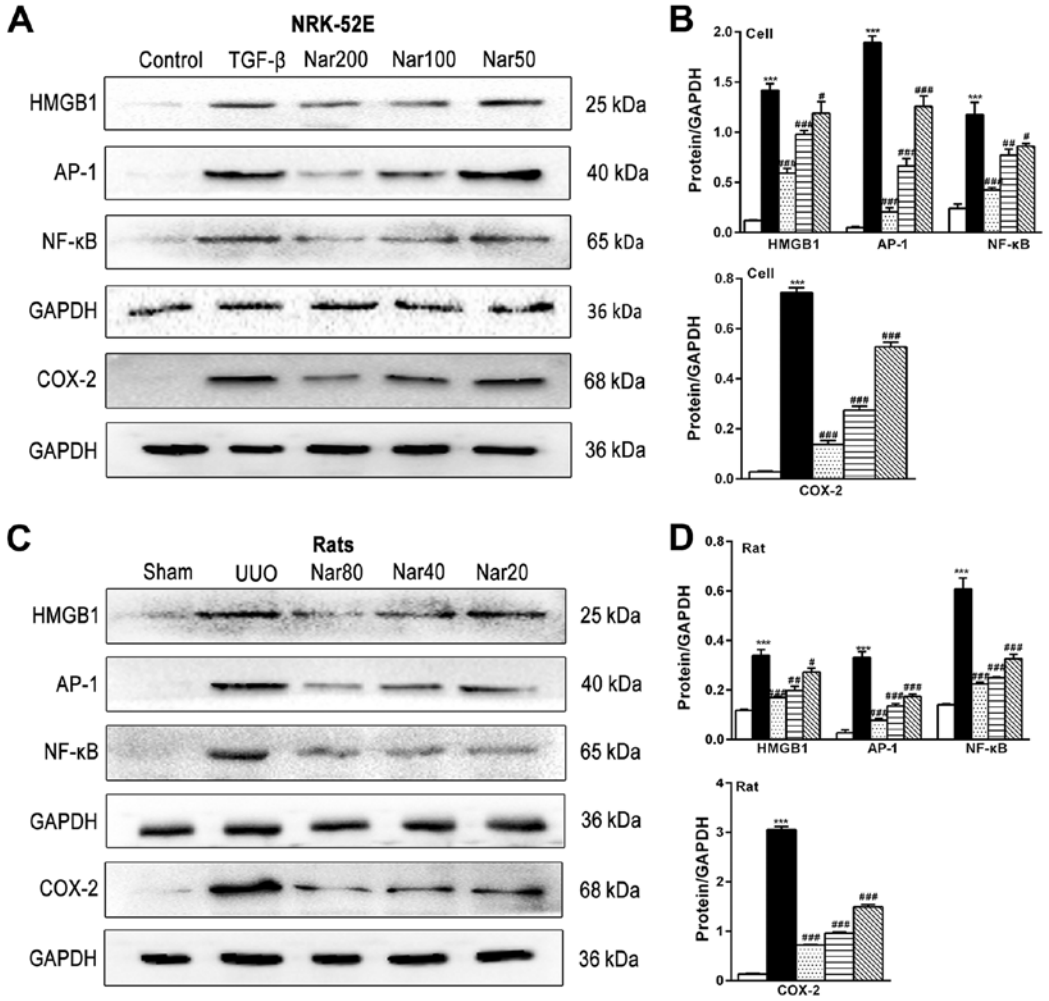

Figure 8. Effects of naringin on the expression of HMGB1, AP-1, NF-κB and COX-2 in NRK-52E cells and rat kidneys. (A) Effect of naringin on HMGB1, AP-1, NF-κB and COX-2 in NRK-52E cells. (B) Quantitative analysis of the protein expression of HMGB1, AP-1, NF-κB and COX-2 in NRK-52E cells. (C) Effect of naringin on HMGB1, AP-1, NF-κB and COX-2 in rat kidneys. (D) Quantitative analysis of the protein expression of HMGB1, AP-1, NF-κB and COX-2 in rat kidneys. Data is presented as mean ± SD (n=6). ***P<0.001 vs. Control; $^{\#}$P<0.05, $^{\#\#}$P<0.01, $^{\#\#\#}$P<0.001 vs. UUO or TGF-β. Nar, naringin; UUO, unilateral ureteral obstruction; HMGB-1, high-mobility group protein B1; COX-2, cyclooxygenase-2; AP-1, activator protein-1; TGF-β, transforming growth factor-β.

The effects of naringin treatment on RIF in rats were subsequently investigated. *In vivo* results showed that naringin administration (20, 40 and 80 mg/kg) reduced the levels of BUN and Scr in the serum samples of UUO rats, improved the dilation or atrophy of renal tubules and reduced the extent of vacuolar degeneration and inflammatory cell infiltration in the kidneys of UUO rats. These observations suggest that naringin can improve renal function and pathological changes in UUO rats. Additionally, naringin reduced collagen fibrous connective tissue proliferation and the deposition of collagen fibers in the kidneys of UUO rats. To evaluate the effect of naringin on RIF in rats further, the expression of fibrosis indicators α-SMA, COL1A1 and COL3A1 was measured. α-SMA expression is an important marker of fibroblasts that also serve a key role in the migratory behavior of fibroblasts (51), whilst COL1A1 and COL3A1 are key components of the skin connective tissue (52). Aberrant expression of COL1A1 and COL3A1 are primary causes of pathological changes in the dermal connective tissue and fibroplasia (53). In the present study, naringin significantly reduced the expression of these three fibrotic markers aforementioned in the kidneys of UUO rats, suggesting that naringin can preserve renal function and inhibit RIF in rats.

TGF-β is a well-studied fibroblast-promoting factor and a powerful anti-inflammatory cytokine that regulates renal inflammation (54-56). It has been previously reported to modulate cell growth, differentiation and proliferation. Overexpression of TGF-β can cause renal fibrosis (57). Results from the present study demonstrated that TGF-β expression in the rat kidney was significantly increased by UUO induction, which was reversed by naringin treatment. This observation suggest that naringin may downregulate the expression of TGF-β in kidney tissues, thus inhibiting RIF. There are ≥9 different isoforms of proteins in the Smad superfamily, which serve as the main intracellular signal transducers of TGF-β (58). Smad2 and Smad3 are receptor-activated Smads that can be activated by TGF-β (59). Following activation, they form complexes with other Smad proteins such as Smad4 to regulate cell cycle progression, cell proliferation, differentiation, adhesion, metastasis, apoptosis and collagen expression (15). By contrast, Smad7 is an inhibitory Smad, which can block receptor-activated Smad

phosphorylation. Smad7 can inhibit the expression of Smad2, Smad3 and Smad4, thereby suppressing and the formation of fibrosis (60). Therefore, the effect of naringin on the TGF-β/Smad signaling pathway was assessed in the present study. Application of TGF-β for inducing cell proliferation *in vitro* is a well-reported method of inducing fibrosis (61,62). Therefore, the present study evaluated the effect of naringin on cell fibrosis following treatment with TGF-β. Naringin could reduce the phosphorylation of Smad2/3 and Smad4 expression whilst increasing the expression of Smad7 in TGF-β-treated NRK-52E cells and kidneys of UUO rats. These findings suggest that naringin can inhibit RIF by regulating the expression of Smad proteins.

In addition to the TGF-β/Smad signaling pathway, Wnt, MAPK and connective tissue growth factor (CTGF) signaling pathways have also been documented to be involved in mediating renal fibrosis and inflammation (63-65). The Wnt signaling pathway is a highly conserved signaling pathway in cells that has been reported to crosstalk with the TGF-β pathway (66). The MAPK pathway consists of a large family of protein kinases, including ERK, JNK/ SAPK, p38 and ERK5/MAPK, and phosphorylated NF-κB after activation of MAPK protein (67). TGF-β forms a positive feedback loop with the MAPK pathway via mitogen-activated protein kinase 7, which is an upstream p38/JNK activator. JNK signaling can enhance the tubular production of thrombospondin-1 which, in turn, activates the latent form of TGF-β (68,69). In addition, it has been revealed that TGF-β can induce the expression of extracellular matrix (ECM) proteins in mesenchymal cells to stimulate the production of protease inhibitors and prevent the enzymatic decomposition of ECM (18). CTGF is induced by TGF-β, which triggers the synthesis of ECM proteins (70). Of note, Smad has been previously demonstrated to lie at the center of an intracellular signaling crosstalk network of Wnt, MAPK and CTGF pathways, to serve an important regulatory role in a number of biological processes (71). Therefore, it could be hypothesized that the anti-fibrotic effects of naringin could be attributed to these three pathways aforementioned.

The occurrence and development of renal fibrosis are not separate processes and involves inflammation. Following the inhibition of AP-1 and NF-κB, the expression of inflammatory cytokines can be inhibited. Inflammatory factors can lead to the increase of stromal cells and intercellular stroma, thus increasing the accumulation of extracellular matrix such as COL1A1 and COL3A1. This is consistent with findings in the present study that the expression of COL1A1 and COL3A1 is increased in fibrotic model cells and kidneys of UUO rats, which was confirmed by the results of Masson and Sirius red staining. These observations showed that naringin can antagonize fibrosis by inhibiting the expression of inflammatory factors.

In conclusion, results from the present study demonstrated that naringin exerted anti-fibrotic effects in the kidney both *in vivo* and *in vitro*, possibly through the TGF-β/Smads signaling pathway whilst suppressing the expression of inflammatory factors. This provides further evidence for the application of naringin as a therapeutic agent for RIF.

Acknowledgements

Not applicable.

Funding

The present study was supported by Liaoning Province's Education Department Program (grant no. L201631), Natural Science Foundation of Liaoning Province (Grant nos. 201602223 and 2019-ZD-0652) and Dalian Medical Science Research Project (grant no. 1912006).

Availability of data and materials

All data generated or analysed during the present study are included in this published article.

Authors' contributions

RCW, GLW, SLY and DSD designed the work; RCW, GLW, TTD, YTL and ZCC collected data; RCW, GLW, SLY and DSD contributed to analysis and interpretation of data. All authors read and approved the final version of the manuscript..

Ethics approval and consent to participate

Ethical approval for the study was granted from the Ethics Committee of Dalian Medical University (Dalian, China).

Patient consent for publication

Not applicable.

Competing interests

The authors declare that they have no competing interests.

References

1. Lawson J, Elliott J, Wheeler-Jones C, Syme H and Jepson R: Renal fibrosis in feline chronic kidney disease: Known mediators and mechanisms of injury. Vet J 203: 18-26, 2015.
2. Kanasaki K, Taduri G and Koya D: Diabetic nephropathy: The role of inflammation in fibroblast activation and kidney fibrosis. Front Endocrinol (Lausanne) 4: 7, 2013.
3. Hill NR, Fatoba ST, Oke JL, Hirst JA, O'Callaghan CA, Lasserson DS and Hobbs FD: Global prevalence of chronic kidney disease-A systematic review and meta-analysis. PLoS One 11: e0158765, 2016.
4. Gewin LS: Renal fibrosis: Primacy of the proximal tubule. Matrix Biol 68-69: 248-262, 2018.
5. Chen PS, Li YP and Ni HF: Morphology and evaluation of renal fibrosis. Adv Exp Med Biol 1165: 17-36, 2019.
6. Wilson PC, Kashgarian M and Moeckel G: Interstitial inflammation and interstitial fibrosis and tubular atrophy predict renal survival in lupus nephritis. Clin kidney J 11: 207-218, 2018.
7. Zhao D and Luan Z: Oleanolic acid attenuates renal fibrosis through TGF-β/Smad pathway in a rat model of unilateral ureteral obstruction. Evid Based Complement Alternat Med 2020: 2085303, 2020.
8. Deng T, Wei Z, Gael A, Deng X, Liu Y, Lai J, Hang L, Yan Q, Fu Q and Li Z: Higenamine improves cardiac and renal fibrosis in rats with cardiorenal syndrome via ASK1 signaling pathway. J Cardiovasc Pharmacol 75: 535-544, 2020.
9. Li W, Cheng F, Songyang YY, Yang SY, Wei J and Ruan Y: CTRP1 attenuates UUO-induced renal fibrosis via AMPK/NOX4 pathway in mice. Curr Med Sci 40: 48-54, 2020.
10. Liu Y, Feng Q, Miao J, Wu Q, Zhou S, Shen W, Feng Y, Hou FF, Liu Y and Zhou L: C-X-C motif chemokine receptor 4 aggravates renal fibrosis through activating JAK/STAT/GSK3β/β-catenin pathway. J Cell Mol Med 24: 3837-3855, 2020.
11. Meng XM, Nikolic-Paterson DJ and Lan HY: TGF-β: The master regulator of fibrosis. Nat Rev Nephrol 12: 325-338, 2016.

12. Tieri P, Termanini A, Bellavista E, Salvioli S, Capri M and Franceschi C: Charting the NF-κB pathway interactome map. PloS One 7: e32678, 2012.
13. Derynck R and Zhang YE: Smad-dependent and Smad-independent pathways in TGF-beta family signalling. Nature 425: 577-584, 2003.
14. Meng XM, Huang XR, Xiao J, Chung AC, Qin W, Chen HY and Lan HY: Disruption of Smad4 impairs TGF-beta/Smad3 and Smad7 transcriptional regulation during renal inflammation and fibrosis in vivo and in vitro. Kidney Int 81: 266-279, 2012.
15. Hu HH, Chen DQ, Wang YN, Feng YL, Cao G, Vaziri ND and Zhao YY: New insights into TGF-β/Smad signaling in tissue fibrosis. Chem Biol Interact 292: 76-83, 2018.
16. Campbell MT, Hile KL, Zhang H, Asanuma H, Vanderbrink BA, Rink RR and Meldrum KK: Toll-like receptor 4: A novel signaling pathway during renal fibrogenesis. J Surg Res 168: e61-69, 2011.
17. Pulskens WP, Rampanelli E, Teske GJ, Butter LM, Claessen N, Luirink IK, van der Poll T, Florquin S and Leemans JC: TLR4 promotes fibrosis but attenuates tubular damage in progressive renal injury. J Am Soc Nephrol 21: 1299-1308, 2010.
18. Jang HR and Rabb H: Immune cells in experimental acute kidney injury. Nat Rev Nephrol 11: 88-101, 2015.
19. Yao L, Li J, Li L, Li X, Zhang R, Zhang Y and Mao X: Coreopsis tinctoria Nutt ameliorates high glucose-induced renal fibrosis and inflammation via the TGF-β1/SMADS/AMPK/NF-κB pathways. BMC Complement Altern Med 19: 14, 2019.
20. Zeng X, Su W, Zheng Y, He Y, He Y, Rao H, Peng W and Yao H: Pharmacokinetics, tissue distribution, metabolism, and excretion of naringin in aged rats. Front Pharmacol 10: 34, 2019.
21. Chen R, Qi QL, Wang MT and Li QY: Therapeutic potential of naringin: an overview. Pharm Biol 54: 3203-3210, 2016.
22. Adil M, Kandhare AD, Ghosh P, Venkata S, Raygude KS and Bodhankar SL: Ameliorative effect of naringin in acetaminophen-induced hepatic and renal toxicity in laboratory rats: Role of FXR and KIM-1. Ren Fail 38: 1007-1020, 2016.
23. El-Desoky AH, Abdel-Rahman RF, Ahmed OK, El-Beltagi HS and Hattori M: Anti-inflammatory and antioxidant activities of naringin isolated from *Carissa carandas* L.: In vitro and in vivo evidence. Phytomedicine 42: 126-134, 2018.
24. Caglayan C, Temel Y, Kandemir FM, Yildirim S and Kucukler S: Naringin protects against cyclophosphamide-induced hepatotoxicity and nephrotoxicity through modulation of oxidative stress, inflammation, apoptosis, autophagy, and DNA damage. Environ Sci Pollut Res Int 25: 20968-20984, 2018.
25. Ahmed S, Khan H, Aschner M, Hasan MM and Hassan STS: Therapeutic potential of naringin in neurological disorders. Food Chem Toxicol 132: 110646, 2019.
26. Dong D, Xu L, Yin L, Qi Y and Peng J: Naringin prevents carbon tetrachloride-induced acute liver injury in mice. J Functional Foods 12: 179-191, 2015.
27. Adil M, Kandhare AD, Visnagri A and Bodhankar SL: Naringin ameliorates sodium arsenite-induced renal and hepatic toxicity in rats: decisive role of KIM-1, Caspase-3, TGF-β, and TNF-α. Ren Fail 37: 1396-1407, 2015.
28. Adil M, Kandhare AD, Ghosh P and Bodhankar SL: Sodium arsenite-induced myocardial bruise in rats: Ameliorative effect of naringin via TGF-β/Smad and Nrf/HO pathways. Chem Biol Int 253: 66-77, 2016.
29. Chen F, Zhang N, Ma X, Huang T, Shao Y, Wu C and Wang Q: Naringin alleviates diabetic kidney disease through inhibiting oxidative stress and inflammatory reaction. PLoS One 10: e0143868, 2015.
30. Wang H, Gao M, Li J, Sun J, Wu R, Han D, Tan J, Wang J, Wang B, Zhang L and Dong Y: MMP-9-positive neutrophils are essential for establishing profibrotic microenvironment in the obstructed kidney of UUO mice. Acta Physiol (Oxf) 227: e13317, 2019.
31. Zhang ZH, He JQ, Zhao YY, Chen HC and Tan NH: Asiatic acid prevents renal fibrosis in UUO rats via promoting the production of 15d-PGJ2, an endogenous ligand of PPAR-γ. Acta Pharmacol Sin 41: 373-382, 2020.
32. Health NIo: Guide for the care and use of laboratory animals. 1985.
33. Hosseinian S, Rad AK, Bideskan AE, Soukhtanloo M, Sadeghnia H, Shafei MN, Motejadded F, Mohebbati R, Shahraki S and Beheshti F: Thymoquinone ameliorates renal damage in unilateral ureteral obstruction in rats. Pharmacol Rep 69: 648-657, 2017.
34. Liu H, Li W, He Q, Xue J, Wang J, Xiong C, Pu X and Nie Z: Mass spectrometry imaging of kidney tissue sections of rat subjected to unilateral ureteral obstruction. Sci Rep 7: 41954, 2017.
35. Livak KJ and Schmittgen TD: Analysis of relative gene expression data using real-time quantitative PCR and the 2(-Delta Delta C(T)) method. Methods 25: 402-408, 2001.
36. Lan HY: Diverse roles of TGF-β/Smads in renal fibrosis and inflammation. Int J Biol Sci 7: 1056-1067, 2011.
37. Boor P and Floege J: Chronic kidney disease growth factors in renal fibrosis. Clin Exp Pharmacol Physiol 38: 441-450, 2011.
38. Nangaku M: Chronic hypoxia and tubulointerstitial injury: A final common pathway to end-stage renal failure. J Am Soc Nephrol 17: 17-25, 2006.
39. Salehi B, Fokou PVT, Sharifi-Rad M, Zucca P, Pezzani R, Martins N and Sharifi-Rad J: The therapeutic potential of naringenin: A review of clinical trials. Pharmaceuticals (Basel) 12: 2019.
40. Zhang M, Guo Y, Fu H, Hu S, Pan J, Wang Y, Cheng J, Song J, Yu Q, Zhang S, *et al*: Chop deficiency prevents UUO-induced renal fibrosis by attenuating fibrotic signals originated from Hmgb1/TLR4/NFκB/IL-1β signaling. Cell Death Dis 6: e1847, 2015.
41. Gong W, Mao S, Yu J, Song J, Jia Z, Huang S and Zhang A: NLRP3 deletion protects against renal fibrosis and attenuates mitochondrial abnormality in mouse with 5/6 nephrectomy. Am J Physiol Renal Physiol 310: F1081-1088, 2016.
42. Chen W, Yan Y, Song C, Ding Y and Du T: Microvesicles derived from human Wharton's Jelly mesenchymal stem cells ameliorate ischemia-reperfusion-induced renal fibrosis by releasing from G2/M cell cycle arrest. Biochem J 474: 4207-4218, 2017.
43. Nogueira A, Pires MJ and Oliveira PA: Pathophysiological mechanisms of renal fibrosis: A review of animal models and therapeutic strategies. In Vivo 31: 1-22, 2017.
44. Xiao Z, Li CW, Shan J, Luo L, Feng L, Lu J, Li SF, Long D and Li YP: Interventions to improve chronic cyclosporine A nephrotoxicity through inhibiting renal cell apoptosis: A systematic review. Chin Med J (Engl) 126: 3767-3774, 2013.
45. Humphreys BD, Xu F, Sabbisetti V, Grgic I, Movahedi Naini S, Wang N, Chen G, Xiao S, Patel D, Henderson JM, *et al*: Chronic epithelial kidney injury molecule-1 expression causes murine kidney fibrosis. J Clin Invest 123: 4023-4035, 2013.
46. Lan HY, Mu W, Tomita N, Huang XR, Li JH, Zhu HJ, Morishita R and Johnson RJ: Inhibition of renal fibrosis by gene transfer of inducible Smad7 using ultrasound-microbubble system in rat UUO model. J Am Soc Nephrol 14: 1535-1548, 2003.
47. Ishii A, Sakai Y and Nakamura A: Molecular pathological evaluation of clusterin in a rat model of unilateral ureteral obstruction as a possible biomarker of nephrotoxicity. Toxicol Pathol 35: 376-382, 2007.
48. Xin BM, Wang XX, Jin W, Yan HM, Cui B, Zhang XW, Hua F, Yang HZ and Hu ZW: Activation of Toll-like receptor 9 attenuates unilateral ureteral obstruction-induced renal fibrosis. Acta pharmacologica Sinica 31: 1583-1592, 2010.
49. Wongmekiat O, Leelarungrayub D and Thamprasert K: Alpha-lipoic acid attenuates renal injury in rats with obstructive nephropathy. BioMed Res Int 2013: 138719, 2013.
50. Lucarelli G, Mancini V, Galleggiante V, Rutigliano M, Vavallo A, Battaglia M and Ditonno P: Emerging urinary markers of renal injury in obstructive nephropathy. BioMed Res Int 2014: 303298, 2014.
51. Shinde AV, Humeres C and Frangogiannis NG: The role of α-smooth muscle actin in fibroblast-mediated matrix contraction and remodeling. Biochim Biophys Acta Mol Basis Dis 1863: 298-309, 2017.
52. Wang Q, Peng Z, Xiao S, Geng S, Yuan J and Li Z: RNAi-mediated inhibition of COL1A1 and COL3A1 in human skin fibroblasts. Exp Dermatol 16: 611-617, 2007.
53. Artlett CM, Sassi-Gaha S, Rieger JL, Boesteanu AC, Feghali-Bostwick CA and Katsikis PD: The inflammasome activating caspase 1 mediates fibrosis and myofibroblast differentiation in systemic sclerosis. Arthritis Rheum 63: 3563-3574, 2011.
54. Zeglinski MR, Hnatowich M, Jassal DS and Dixon IM: SnoN as a novel negative regulator of TGF-β/Smad signaling: A target for tailoring organ fibrosis. Am J Physiol Heart Circ Physiol 308: H75-H82, 2015.
55. Gu YY, Liu XS, Huang XR, Yu XQ and Lan HY: Diverse role of TGF-β in kidney disease. Front Cell Dev Biol 8: 123, 2020.
56. Zhang X, Huang H, Zhang G, Li D, Wang H and Jiang W: Raltegravir attenuates experimental pulmonary fibrosis in vitro and in vivo. Front Pharmacol 10: 903, 2019.
57. ten Dijke P and Hill CS: New insights into TGF-β-Smad signalling. Trends Biochem Sci 29: 265-273, 2004.

58. Miyazawa K, Shinozaki M, Hara T, Furuya T and Miyazono K: Two major Smad pathways in TGF-beta superfamily signalling. Genes Cells 7: 1191-1204, 2002.
59. Biernacka A, Dobaczewski M and Frangogiannis NG: TGF-β signaling in fibrosis. Growth Factors 29: 196-202, 2011.
60. Yan X, Liao H, Cheng M, Shi X, Lin X, Feng XH and Chen YG: Smad7 protein interacts with receptor-regulated smads (R-Smads) to inhibit transforming growth factor-β (TGF-β)/smad signaling. J Biol Chem 291: 382-392, 2016.
61. Masola V, Carraro A, Granata S, Signorini L, Bellin G, Violi P, Lupo A, Tedeschi U, Onisto M, Gambaro G and Zaza G: In vitro effects of interleukin (IL)-1 beta inhibition on the epithelial-to-mesenchymal transition (EMT) of renal tubular and hepatic stellate cells. J Transl Med 17: 12, 2019.
62. Liu JH, He L, Zou ZM, Ding ZC, Zhang X, Wang H, Zhou P, Xie L, Xing S and Yi CZ: A novel inhibitor of homodimerization targeting MyD88 ameliorates renal interstitial fibrosis by counteracting TGF-β1-induced EMT in vivo and in vitro. Kidney Blood Press Res 43: 1677-1687, 2018.
63. Edeling M, Ragi G, Huang S, Pavenstadt H and Susztak K: Developmental signalling pathways in renal fibrosis: The roles of Notch, Wnt and Hedgehog. Nature Rev Nephrol 12: 426-439, 2016.
64. Wang D, Warner GM, Yin P, Knudsen BE, Cheng J, Butters KA, Lien KR, Gray CE, Garovic VD, Lerman LO, *et al*: Inhibition of p38 MAPK attenuates renal atrophy and fibrosis in a murine renal artery stenosis model. Am J Physiol Renal Physiol 304: F938-F947, 2013.
65. Ito Y, Aten J, Bende RJ, Oemar BS, Rabelink TJ, Weening JJ and Goldschmeding R: Expression of connective tissue growth factor in human renal fibrosis. Kidney Int 53: 853-861, 1998.
66. Caraci F, Gili E, Calafiore M, Failla M, Rosa CL, Crimi N, Sortino MA, Nicoletti F, Copani A and Vancheri C: TGF-beta1 targets the GSK-3beta/beta-catenin pathway via ERK activation in the transition of human lung fibroblasts into myofibroblasts. Pharmacol Res 57: 274-282, 2008.
67. Qi W, Twigg S, Chen X, Polhill TS, Poronnik P, Gilbert RE and Pollock CA: Integrated actions of transforming growth factor-beta1 and connective tissue growth factor in renal fibrosis. Am J Physiol Renal Physiol 288: F800-F809, 2005.
68. Naito T, Masaki T, Nikolic-Paterson DJ, Tanji C, Yorioka N and Kohno N: Angiotensin II induces thrombospondin-1 production in human mesangial cells via p38 MAPK and JNK: A mechanism for activation of latent TGF-beta1. Am J Physiol Renal Physiol 286: F278-F287, 2004.
69. Gao Y, Jiang W, Dong C, Li C, Fu X, Min L, Tian J, Jin H and Shen J: Anti-inflammatory effects of sophocarpine in LPS-induced RAW 264.7 cells via NF-κB and MAPKs signaling pathways. Toxicol In Vitro 26: 1-6, 2012.
70. Ihn H: Pathogenesis of fibrosis: Role of TGF-beta and CTGF. Curr Opin Rheumatol 14: 681-685, 2002.
71. Luo K: Signaling cross talk between TGF-beta/Smad and other signaling pathways. Cold Spring Harb Perspect Biol 9: a022137, 2017.